Identification of an Additional Low-Lying Excited State of Carotenoid Radical Cations

Sergiu Amarie, Kibrom Arefe, Jan Hendrik Starcke, Andreas Dreuw, and Josef Wachtveitl*

Institute of Physical and Theoretical Chemistry, Goethe-University Frankfurt, Max von Laue-Strasse 7, 60438 Frankfurt am Main, Germany

Received: July 8, 2008; Revised Manuscript Received: August 28, 2008

Carotenoids are the crucial pigments involved in photoprotection and in scavenging harmful free radicals in all living organisms. The underlying chemical processes are charge transfer and free radical reactions, both of them leading to carotenoid radical cation ($Car^{\bullet+}$) formation. Accurate knowledge of the molecular properties of $Car^{\bullet+}$ is thus a prerequisite for understanding of their function as photoprotective and antioxidant agents. Despite their fundamental importance in nonphotochemical quenching in green plants, only little is known about the $Car^{\bullet+}$ excited states and their dynamics. Our combined experimental and theoretical investigation employing femtosecond time-resolved pump−probe spectroscopy and quantum chemical calculations proves the existence of a second low-lying $\pi\pi^*$ excited-state energetically below the well-known strongly allowed excited-state responsible for the intense absorption of $Car^{\bullet+}$ in the near-IR region. Hence, we suggest denoting the latter state as D_3 state in the future. Our findings have also implications for nonphotochemical quenching in green plants, since direct quenching of chlorophyll excited states by Förster energy transfer to $Car^{\bullet+}$ is possible and efficient.

Introduction

Carotenoids (Car) fulfill important functions in light harvesting and photoprotection and are well-known as antioxidants. As photoprotective pigments, they scavenge dangerous singlet oxygen molecules and quench both singlet and triplet states of electronically excited chlorophylls (Chls).[1−5] The fundamental molecular processes underlying these functions are energy and electron transfer between Cars and Chls.[6,7] In addition, Cars are recognized to play important roles as potent scavengers of free radicals preventing human diseases that are believed to be initiated by free radicals.[8] The mechanism of the reaction is given by

$$R^{\bullet} + Car \rightarrow R^{-} + Car^{\bullet+}$$

While β-carotene (β-Car) is a very important protective agent in almost all living organisms, one of the important functions of zeaxanthin and lutein (Lut) is protection of the retina against photo-oxidation. The retina is the only organ in the body which is continually exposed to high levels of focused radiation and which is in a highly oxygenated environment. This combination of light and oxygen, together with the presence of photosensitizers, provides the basis for oxygen free radical and singlet oxygen generation. Lut and zeaxanthin play particularly efficient roles in scavenging these free radicals and in dissipating excess energy off the retina via generation of carotenoid radical cations ($Car^{\bullet+}$).[9] Therefore, detailed knowledge of the optical and kinetic properties of the $Car^{\bullet+}$ and, in particular, of their excited electronic states is essential to achieve a detailed understanding of these processes.

One of the central functions of Cars, extensively studied yet poorly understood at the molecular level, is the quenching of Chl singlet excited states in photosynthetic systems under high-light conditions, when the harvested energy exceeds the turnover capacity of the reaction center.[4,10,11] It has been observed that photosynthetic systems can adapt to high levels of light by switching to specific states,[11] which safely dissipate excess energy as heat. In green plants, for example, this process is known as nonphotochemical quenching (NPQ). Recently, the so-called energy-dependent quenching component qE of NPQ has been in the focus of photosynthesis research.[12−19] At present, neither the exact location of qE nor the detailed molecular mechanism are known and are thus matter of an ongoing debate.[16−20] On the basis of recent quantum chemical calculations and elaborate time-resolved spectroscopic experiments, an NPQ mechanism has been proposed in which $Car^{\bullet+}$ formation is the terminal quenching step via electron transfer from Car to Chl.[16,21] Along this line of research, $Car^{\bullet+}$ have recently been observed in several photosynthetic pigment protein complexes, including bacterial light-harvesting complexes (LHC) LH2[22,23] and isolated plant LHCs supporting the above-described mechanism of qE.[12,13,19]

Nevertheless, only little is known about the optical properties of the $Car^{\bullet+}$, the energetic positions of their excited states, and their interaction with neighboring photosynthetic pigments.

Hence, a detailed knowledge of the excited-state properties of $Car^{\bullet+}$ is a step forward not only in understanding natural photosynthetic processes but also in studying and designing artificial photosynthetic systems.[24−26] In artificial systems, the key step is efficient photoinduced electron transfer eventually producing a final charge-separated state. Cars are excellent candidates for the design of such artificial systems due to their low ionization potential, which makes them excellent electron donors.[27,28]

In this work, we present a combined experimental and theoretical investigation of the excited-state properties of Lut and β-Car radical cations by means of time-resolved transient absorption (TA) spectroscopy and quantum chemical calculations. As a first step, static absorption spectra are recorded and

* To whom correspondence should be addressed. Tel.: +49 (0)69 798 29351. Fax: +49 (0)69 798 29709. E-mail: wveitl@theochem.uni-frankfurt.de.

10.1021/jp806030y CCC: $40.75
Published on Web 10/09/2008

their dependence on the solvent properties is discussed. Most importantly, our pump−probe experiments reveal the existence of a new low-lying excited-state in $Car^{\bullet+}$, which is corroborated by quantum chemical calculations. On the basis of our findings, a simple mechanism for quenching of Chl excited states is proposed, which has important implications for NPQ in photosynthetic organisms.

Materials and Methods

Sample Preparation. Lut and β-Car was purchased from Sigma and stored at −20 °C. Chloroform, acetonitrile, and CS2 were also purchased from Sigma. To obtain the desired cation concentration and to avoid formation of carotenoid dications, equal amounts of 0.5 M FeCl3 were added to 1 M Car. For the time-resolved experiments, the typical sample OD was 0.6/mm at 935 nm. Sample stability was confirmed by measuring the absorption spectra before and after the time-resolved measurements. The samples were prepared under Ar atmosphere to prevent reaction with oxygen. However, a decrease of 10% of the cation band between the spectrum before and after the ultrafast measurements was observed.

Steady State Absorption. Absorption spectra of the $Car^{\bullet+}$ were recorded at room temperature using a Jena-Specord S100 photodiode array spectrometer for measurements up to 1020 nm and a Jasco V 670 spectrometer to cover the spectral range above 1000 nm.

Time-Resolved Absorption Spectroscopy. The time-resolved measurements were performed using a CLARK CPA 2001 (Dexter, MI) laser/amplifier system operating at a repetition rate of ∼1 kHz at a central wavelength of 775 nm.[29,30] The chemically generated carotenoid radical cations were excited by pulses generated using a noncollinear optical parametric amplifier (NOPA) with the output tuned to 935 nm for which the maximum excitation energy was kept at 30 nJ. For the probe pulses a white light continuum was generated by focusing amplified 775 nm light into a 5 mm sapphire window. To select the spectral region of interest in the near-IR, a RG 830 filter was used. Femtosecond time delays between pump and probe were controlled by a translation stage covering delay times up to 1.5 ns. To minimize accumulation of photoproducts, the sample was translated continuously both horizontally and vertically in a direction normal to the bisector of the pump and probe beams at ∼10 cm/s.

Computational Details. The computational investigation of the radical cations of Lut and β-Car comprises optimization of their ground-state equilibrium geometries using conventional density functional theory (DFT)[31] as well as calculation of the vertical excited states employing time-dependent DFT (TDDFT)[32,33] with the standard B3LYP[34] exchange-correlation functional and the 6-31G* basis set as implemented in the Q-Chem 3.0 package of quantum chemistry programs.[35] For the analysis of the nature of the excited states, the corresponding detachment and attachment densities have been calculated.[36,37] The detachment density corresponds to the density that is removed from the ground-state density upon the excitation, while the attachment density is added upon excitation. These densities allow for an easy interpretation of excited states even when the excitation is a complicated mixture of many determinants.

While for neutral Cars it has been shown that the inclusion of doubly excited states is crucial for a proper description of the lowest excited S_1 state,[38,39] high-level computations with the extended algebraic diagrammatic construction scheme of second order (ADC(2)-x)[40,41] on radical cations of linear polyenes with up to eight conjugated double bonds have shown that doubly excited configurations do not play important roles for the lowest excited states of $Car^{\bullet+}$. Thus, TDDFT calculations are much better suited for the description of radical cations of Cars than for neutral ones. However, $Car^{\bullet+}$ possess an odd number of electrons and are therefore generally subject to an unrestricted treatment. At the Hartree−Fock level one observes a large amount of spin contamination in the electronic ground state. Through the use of DFT, the spin contamination vanishes and one obtains values of 0.81 for the expectation value of $\hat{S}^2$ for both $Lut^{\bullet+}$ and β-$Car^{\bullet+}$, which is very close to the correct one of 0.75.

Results and Discussion

Optical Properties of Lutein and β-Carotene Radical Cations. Generation and detection of $Car^{\bullet+}$ can be achieved by several optical methods both in solution and directly in the protein environment. Typically, photoionization techniques exploit one-photon excitation into higher autoionizing Car excited states;[42−44] however, $Car^{\bullet+}$ generation employing two-photon ionization has recently been reported.[12] Two photons of lower energy have the great advantage that experiments can be performed in the natural biological environment without large perturbation of the natural situation. Nevertheless, all these methods only lead to short-lived populations of $Car^{\bullet+}$ species, which decay within microseconds to milliseconds due to charge recombination. In contrast, chemical oxidation is an attractive and simple method to generate long-lived $Car^{\bullet+}$ molecules,[45,46] which are stable for hours and decay essentially only by reaction with O_2. Pump−probe spectroscopy can then be easily applied to study excited-state dynamics. The oxidizing agent used in this work is ferric chloride ($FeCl_3$), which reacts with the neutral Car and leads to the formation of the $Car^{\bullet+}$.

$$Car + Fe^{III}Cl_3 \rightarrow Car^{\bullet+} + Fe^{II}Cl_2 + Cl^-$$

The formation of $Car^{\bullet+}$ was initiated by addition of $FeCl_3$ solution to the Car solution and was monitored by changes in the absorption spectrum of the Car and its radical cation (Figure 1A). When equal amounts of 0.5 M $FeCl_3$ were added to 1 M β-Car donor solution, the concentration of the neutral compound decreased by a factor of 2 which is seen as a decrease of the intensity of the $S_0 \rightarrow S_2$ transition of the neutral Car at $\lambda_{max} =$ 463 nm. At the same time, an absorption signal emerged at $\lambda_{max} =$ 975 nm which is attributed to the formation of $Car^{\bullet+}$.

Following this protocol, room temperature absorption spectra of β- $Car^{\bullet+}$ have been measured in solvent with decreasing polarity measured by the dielectric constant ε and with increasing polarizability α (acetonitrile ($\varepsilon = 37.5$, $\alpha = 4.48$ Å^3), chloroform ($\varepsilon = 4.8$, $\alpha = 8.2$ Å^3), and CS_2 ($\varepsilon = 2.6$, $\alpha = 8.74$ Å^3)) and are displayed in the inset of Figure 1A. Although a number of other ways to determine polarity have been described, for example, the *Y* scale, a quantitative measure for the ionization power of solvents, the *Z* value solvent polarity scale or the $E_T(30)$ value, which relies on the measurement of the absorption maximum of a charge transfer complex, we focus here on the more commonly used dielectric constant.

The spectra were taken immediately after adding the $FeCl_3$ solution. To facilitate the comparison, the $Car^{\bullet+}$ spectra have been normalized to the same absorbance value at the wavelength of maximum absorption. It is apparent that the absorption band of the β-$Car^{\bullet+}$ exhibits a significant spectral shift: its λ_{max} value shifts to lower energy, that is, longer excitation wavelengths with decreasing polarity and increasing polarizability of the

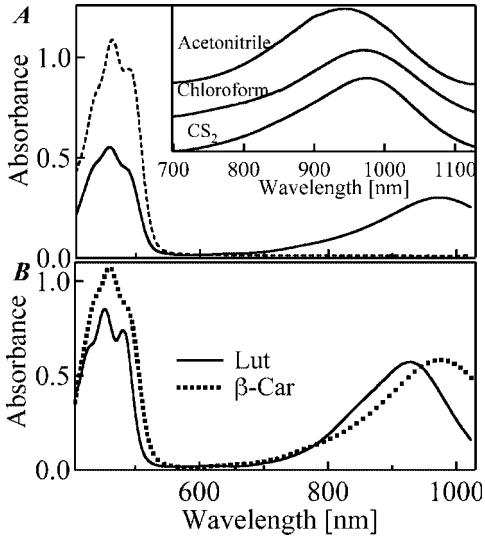

Figure 1. Optical absorption of lutein and β-carotene radical cations. (A) Neutral β-carotene (dotted line) and β-carotene radical cation (solid line) recorded upon addition of 0.5 M equivalent of $FeCl_3$ in chloroform. (B) Lutein radical cation (solid line), and β-carotene radical cation (dotted line) prepared as in panel A. Optical absorption of β-carotene radical cation in different solutions: acetonitrile chloroform and CS_2 (inset A).

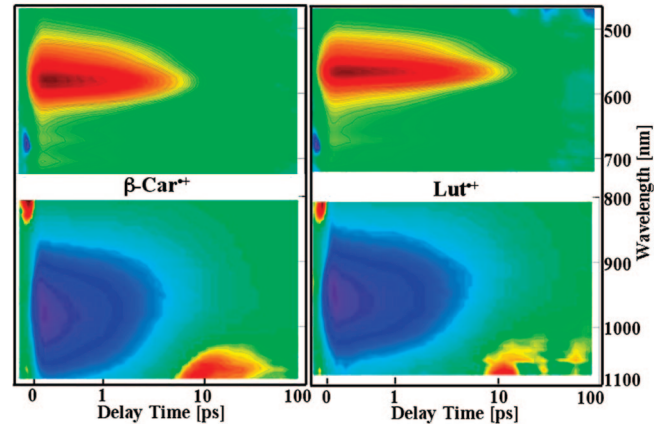

Figure 2. Two-dimensional plot of the transient absorption data of lutein and β-carotene radical cations upon excitation at 935 nm.

solvent. In detail, from acetonitrile to CS_2 the band shifts by about 35 nm reflecting the Car-solvent interaction (Figure 1A). The β-Car$^{\bullet+}$ bands have maxima located at 940 nm in acetonitrile, 970 nm in chloroform, and 975 nm in CS_2. Previous measurements revealed that the β- Car$^{\bullet+}$ has its absorption maximum at 920 nm in ethanol,[12] at 935 nm in acetonitrile,[46] at 970 nm in dichloromethane,[45] and at about 1000 nm in PS II.[47] Although it is in principle difficult to distinguish between the influence of the polarity and polarizability of the solvent, it appears that the polarizability of the solvent is the relevant quantity determining the spectral shift. The trend of the observed shifts is better described by the trend of the polarizabilities than by the one of the dielectric constants. Also in previous studies, the modulation of the spectral shift of the Car$^{\bullet+}$ absorption band has been assigned to the polarizability of the solvent.[48]

Comparison of the maximum absorption wavelengths of Lut$^{\bullet+}$ and β-Car$^{\bullet+}$ in chloroform reveals a shift of the absorption band toward lower energies from Lut$^{\bullet+}$ (927 nm) to β-Car$^{\bullet+}$ (970 nm) (Figure 1B). This shift is well known to occur due to the difference in conjugation length of the carotenoids and is thus a direct consequence of the shorter conjugated chain length of Lut compared with β-Car, which is in nice agreement with previous reports.[12,49]

In summary, the wavelength of the Car$^{\bullet+}$ absorption band in the near-IR region is most notably influenced by the polarizability of the solvent and the number of conjugated double bonds of the Car. When the conjugation length of a Car is known, it may serve as a sensor for the polarizability of the environment.

Excited State Dynamics of Carotenoid Radical Cations. To investigate the properties and in particular the lifetimes of the low-lying excited states of the radical cations of Lut and β-Car, TA spectra were measured using a high intensity pump pulse centered at 935 nm and a broadband white-light probe pulse which spans two spectral regions (400−700 and 800−1100 nm). TA spectra of Lut$^{\bullet+}$ and β-Car$^{\bullet+}$ were recorded in chloroform upon excitation into the strongly one-photon allowed state absorbing around 950 nm. In previous works, this state is commonly referred to as D_2 excited state,[28,45,50,51] in analogy to the S_2 state of neutral Cars. Our computations will later reveal that for Lut$^{\bullet+}$ and β-Car$^{\bullet+}$ this state corresponds to the third lowest excited-state of the Car$^{\bullet+}$ and will thus be denoted as D_3 in the following.

There are three distinct regions observed in the time-resolved TA spectra (Figure 2): the ground-state bleach around 950 nm stemming from the depopulation of the ground-state by the initial pump pulse, and two excited-state absorption (ESA) bands, one in the visible region around 570 nm and one above 1000 nm. In analogy to the steady state spectra shown in Figure 1B, where the absorption bands of Car$^{\bullet+}$ shift to longer wavelengths with increasing number of conjugated double bonds, the main positive absorption band in the time-resolved spectra shown in Figure 2 also shifts to lower energies from 566 nm for Lut$^{\bullet+}$ to 582 nm for β-Car$^{\bullet+}$. Similarly, the weaker ESA in the near-IR region also shows a red-shift of 16 nm from Lut$^{\bullet+}$ (1040 nm) to β-Car$^{\bullet+}$ (1056 nm). Previous analogous experiments on neutral Cars have revealed similar red-shifts for the dominating ESA bands corresponding to the $S_1 \rightarrow S_N$ transition with increasing conjugation length of xanthophyll Cars.[52,53]

To explore in more detail the photoinitiated processes, that is, the lifetime and decay pathways of the initial excited-state population, the temporal evolution of the absorption spectrum was analyzed at the maximum of the ESA bands and at the minimum of the ground-state bleach (Figure 3). The corresponding kinetic traces measured at 568 nm (Lut$^{\bullet+}$) and 582 nm (β-Car$^{\bullet+}$) are displayed in Figure 3, top. They contain large positive signals which appear within the first 200 fs and decay exponentially in two steps. The lifetime of β-Car$^{\bullet+}$ is shorter than the one of Lut$^{\bullet+}$, which might be related to the number of conjugated double bonds. The second kinetic traces shown in Figure 3 (middle) were selected at the minima of the ground-state bleach signals, that is, at 968 nm for Lut$^{\bullet+}$ and 992 nm for β-Car$^{\bullet+}$ and both are dominated by large negative signals. The ground-state recovery of β-Car$^{\bullet+}$ proceeds slightly faster than the one of Lut$^{\bullet+}$. For the last set of kinetic traces recorded 1040 nm (Lut$^{\bullet+}$) and 1056 nm (β-Car$^{\bullet+}$) (Figure 3, bottom), we observe a rapidly formed negative signal, which decays within the first few picoseconds followed by a weak positive transient signal with a maximum at about 10 ps after excitation Also in this spectral region, the excited-state dynamics of β-Car$^{\bullet+}$ seems to proceed slightly faster than for Lut$^{\bullet+}$.

The time-resolved TA spectra have been analyzed with a global exponential fit procedure. This allows us to relate the observed kinetics to individual excited-state populations with distinct lifetimes and spectral features. Figure 4 shows the

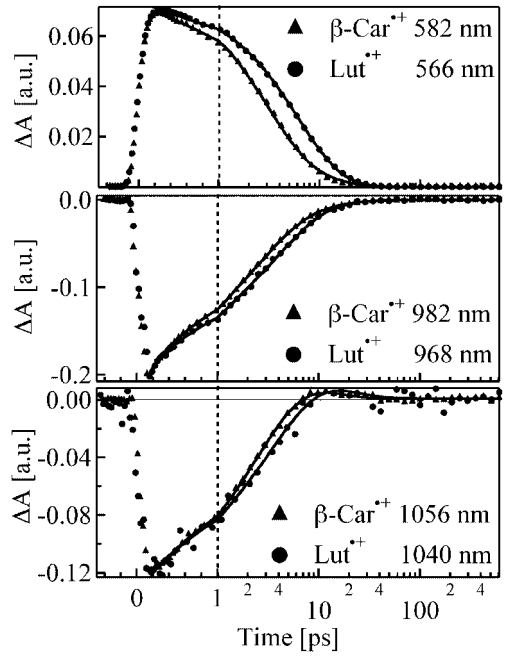

Figure 3. Transient absorption kinetic traces of lutein (circles) and β-carotene (triangles) radical cations probed at the $D_2 \rightarrow D_M$ ESA maxima (top panel), at the ground-state bleach minima (middle panel), and at the $D_1 \rightarrow D_N$ ESA maxima (bottom panel) after excitation to 935 nm.

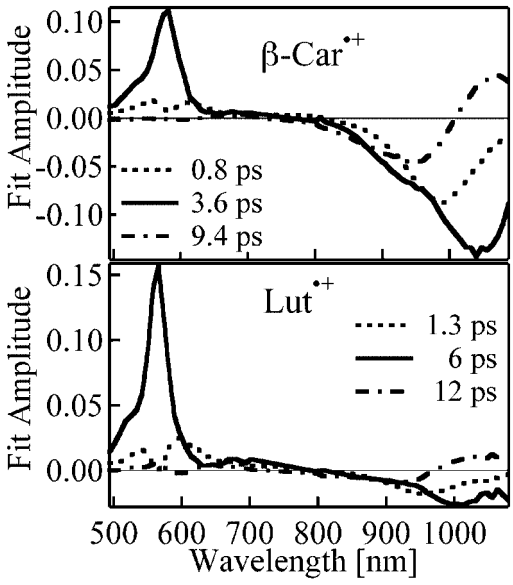

Figure 4. Amplitude spectra represented by the global fit amplitude of β-carotene (top panel) and lutein (bottom panel) radical cations upon 935 nm excitation.

resulting amplitude spectra of the global exponential fit of the TA spectra of β-Car$^{\bullet+}$ and Lut$^{\bullet+}$. For both Car$^{\bullet+}$, three components were necessary to obtain satisfactory fits. According to the fit, the experimentally observed excited-state dynamics of the investigated Car$^{\bullet+}$ can be described with the following three kinetic components: (1) a fast component τ_1 with a time constant of 0.8 ps for β-Car$^{\bullet+}$ and 1.3 ps for Lut$^{\bullet+}$, which has spectral features of Car$^{\bullet+}$ ground-state bleach corresponding to negative absorption centered around 950 nm and which exhibits a positive amplitude due to ESA between 500 and 700 nm. These spectral shapes and lifetimes can be interpreted as an ultrafast radiationless transition from the initially populated excited-state into an energetically lower lying excited state. (2)

TABLE 1: Excitation Energies, Oscillator Strength, and Nature of the Five Lowest Excited States of the Radical Cations of Lutein and B-Carotene at the Theoretical Level of TDDFT/B3LYP/6-31G*

	β-Carotene			Lutein		
	E_{ex} [eV] (Osc.)	E_{ex} [nm]	nature	E_{ex} [eV] (Osc.)	E_{ex} [nm]	nature
D_1	0.90 (0.05)	1378	$\pi\pi^*$	0.95 (0.03)	1306	$\pi\pi^*$
D_2	1.44 (0.00)	862	$\pi\pi^*$	1.51 (0.59)	821	$\pi\pi^*$
D_3	1.50 (3.62)	827	$\pi\pi^*$	1.61 (2.82)	770	$\pi\pi^*$
D_4	1.75 (0.00)	709	$\pi\pi^*$	1.68 (0.26)	738	CT
D_5	2.01 (0.25)	617	$\pi\pi^*$	1.89 (0.12)	656	$\pi\pi^*$

The second component τ_2 has the largest amplitude and possesses time constants of 3.6 ps for β-Car$^{\bullet+}$ and 6 ps for Lut$^{\bullet+}$. The corresponding amplitude spectra show a strong ESA at 582 nm for β-Car$^{\bullet+}$ and 566 nm for Lut$^{\bullet+}$ together with a broad negative profile which spans the spectral range above 800 nm, red-shifted compared to the first component by about 50 nm. The negative amplitude of this component can be interpreted as on the one hand ground-state recovery, which will give negative contributions to the amplitude around 950 nm, and on the other as a growing ESA signal of some other new excited-state above 1000 nm. Together these two contributions result in the broad negative band of the second component displayed in Figure 4. (3) The third kinetic component τ_3 has time constants of 9.4 and 12 ps for β-Car$^{\bullet+}$ and Lut$^{\bullet+}$, respectively. The corresponding amplitude spectra are overall similar, although the amplitude of the Lut$^{\bullet+}$ spectrum is significantly smaller than the one of β-Car$^{\bullet+}$. However, both amplitude spectra consist of a negative signal around 950 nm, a sign change and a positive band above 1000 nm. This shape is typical for ground-state recovery stemming from the decay of the new additional excited-state previously populated with time constant τ_2.

In summary, the global fit analysis reveals three excited states to be involved in the observed excited-state dynamics of β-Car$^{\bullet+}$ and Lut$^{\bullet+}$ The initially excited-state D_3 decays rapidly with a time-constant of about one picosecond into a lower lying state D_2. The latter state possesses two possibilities to decay within about 5 ps: via transition to the ground-state D_0 and or to a second low-lying excited-state D_1. Finally the D_1 state returns to the ground-state with a time constant of about 10 ps. From the analysis of our experimental data it is clear that the investigated two Car$^{\bullet+}$ possess two excited states with different spectral properties and lifetimes below the well-known state absorbing in the NIR region.

Nature of the Low Lying Excited States of Carotenoid Radical Cations. To corroborate our experimental identification of the new excited-state and to characterize its nature, quantum chemical calculations have been performed on the excited states of the cation radicals of Lut and β-Car. As first step of the theoretical investigation, the ground-state structures have been optimized at the theoretical level of DFT/B3LYP/6-31G*. Both species possess an unpaired electron and thus a doublet ^2A_u-type electronic ground-state in C_{2h} symmetry of linear polyenes. At the equilibrium ground-state geometries, the five lowest vertical excited states of the Car$^{\bullet+}$ of Lut and β-Car have been computed. Both carotenoid radical cations exhibit strongly allowed D_3 excited states with excitation energies of 1.50 and 1.61 eV, respectively (Table 1). In agreement with our previous experimental observation, the D_3 state is red-shifted for β-Car$^{\bullet+}$ compared to Lut$^{\bullet+}$ by 0.11 eV at the applied theoretical level, which is due to the shorter conjugation length of Lut (10)

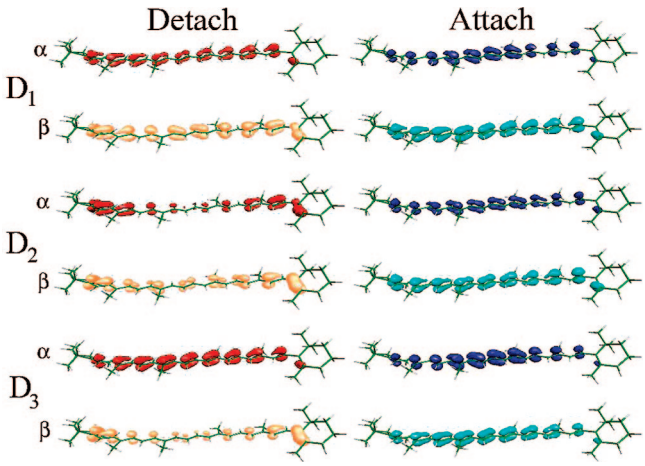

Figure 5. Nature of the three lowest excited states of the β-carotene radical cation represented as detachment/attachment density plots of the α and β parts of the ground-state wave function.

compared to β-Car (11). These states correspond to $\pi\pi^*$ excited states with ^2B_g pseudosymmetry in C_{2h} resulting in an allowed D_0 (^2A_u) → D_3 (^2B_g) transition. Due to the higher symmetry of β-Car compared to Lut, the symmetry classification is more appropriate for the former than for the latter. The nature of these states is most easily represented by detachment/attachment plots of the α and β electron densities (Figure 5). These densities correspond to those parts of the electron density which are removed and attached to the ground-state electron density upon excitation. The symmetry of the attachment−detachment densities determines the selection rules in analogy to the orbitals in the single-particle picture. Both β-Car$^{\bullet+}$ and Lut$^{\bullet+}$ possess two lower lying excited $\pi\pi^*$ states D_1 (^2B_g) and D_2 (^2A_u) at 0.90 and 0.95 eV and at 1.44 and 1.51 eV, respectively. In the case of β-Car$^{\bullet+}$, the D_1 state has a small oscillator strength of 0.05 while the D_2 state is practically symmetry forbidden. Also the D_1 state of Lut$^{\bullet+}$ is weakly allowed. However, since the spatial C_{2h} symmetry is much less conserved in Lut$^{\bullet+}$ and the D_2 and D_3 state are very close in energy (0.1 eV), one observes configuration mixing between these states in Lut$^{\bullet+}$ which results in an oscillator strength of 0.59 for the D_2 state of Lut$^{\bullet+}$. The lower-symmetry of lutein, showing considerable intensity borrowing, suggests strong vibronic couplings in β-Car$^{\bullet+}$. This might lead to population of other states (e.g., D_2 and D_4) which are nearly degenerate with D_3. However, this has no implications for the proposed mechanism, since the general picture of the deactivation mechanism is hardly expected to change due to vibronic coupling. The electronic structure of the D_1 and D_2 states of both Car$^{\bullet+}$ though are essentially identical since they possess essentially equivalent detachment/attachment densities. The detachment/attachment density-plots are shown for β-Car$^{\bullet+}$ in Figure 5.

Compared to the neutral β-Car and Lut, the excited states of the Car$^{\bullet+}$ are substantially red-shifted. For example, the S_2 $\pi\pi^*$ state of β-Car corresponding to the highest occupied molecular orbital (HOMO)−lowest unoccupied molecular orbital (LUMO) single-electron transition exhibits an excitation energy of about 2.3 eV at the level of TDDFT/B3LYP/6-31G*. The strong decrease of the excitation energy upon ionization results on one hand from the positive charge of the cations leading to a reduced HOMO−LUMO gap. On the other hand, removing one electron from the HOMO orbital of the neutral Car to generate the cation allows for a new additional excitation of an electron from the former HOMO-1 into the now singly occupied former HOMO. This electronic transition exhibits a small excitation energy and

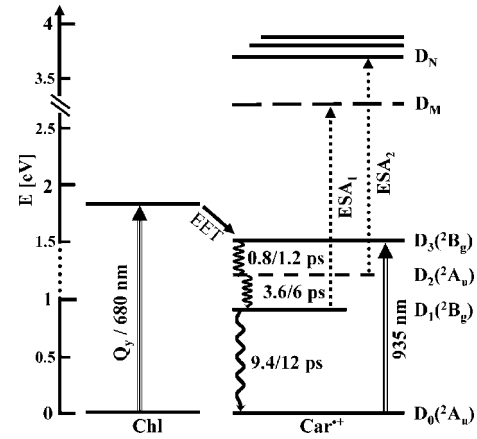

Figure 6. Energy level diagram depicting relaxation processes that occur after photoexcitation of lutein/β-carotene radical cations. Double arrow represents excitation of the D_3 state, dotted arrows corresponds to excited-state transitions of D_1→D_M (ESA_1) and D_2→D_N (ESA_2), while wavy arrows denote intramolecular relaxation processes. The processes described in this study are labeled by their corresponding time constant. Excitation of chlorophylls into the first excited state (Q_y transition) leads to efficient excitation energy transfer (EET) to D_3 excited state. The area between 1 and 1.5 eV is not plotted to scale to improve graphics (see Table 1 for exact values). See the text for details.

since it mixes with all ^2B_g symmetric states of the Car$^{\bullet+}$ and thus lowers their total energy, their excitation energies are particularly decreased.

Energetically above the D_3 state, one finds a plethora of excited $\pi\pi^*$ states, which at higher energies are very close in energy. Unfortunately, the transition dipoles between D_3 and other excited states are not computed/analyzed since this theoretical methodology is not available. For β-Car$^{\bullet+}$, the D_4 and D_5 excited states appear at 1.75 and 2.01 eV, which both exhibit pseudo ^2B_g symmetry. In the case of Lut$^{\bullet+}$ one finds a $n\pi^*$ state as D_4 which has substantial charge-transfer (CT) character. Here an electron of the lone pair of one hydroxy group is excited into the π-system. Because of the well-known CT failure of TDDFT this state is computed at too low energy and thus can be excluded from further discussions.[54,55] The D_5 state of lutein is again a $\pi\pi^*$ state and corresponds to the D_4 state of the β-Car$^{\bullet+}$.

Previous early calculations gave no evidence of the existence of two low-lying excited states below the well-known allowed state.[50,56] Only one forbidden D_1 and the well-known allowed state (D_2 at that time) were found. However, indications were given that for longer polyenes an additional optically forbidden state of ground-state symmetry may drop in energy and become the D_2 state. Indeed, our experiments and the new quantum chemical calculations, now clearly demonstrate the existence of two excited states below the strong allowed state in the Lut$^{\bullet+}$ and β-Car$^{\bullet+}$.

The quantum chemical calculations of energetically higher-lying excited states of the Car$^{\bullet+}$ is of no help in the interpretation of the ESA signals, since the error in the excitation energy and concomitantly the density of state increases at higher excitation energies making it impossible to assign one particular state to the ESA from D_3, D_2, or D_1. Nevertheless, from these computations it is clear that many excited states exist that can account for the observed ESA signals. Since the D_1 and D_2 states possess different spatial symmetry ^2B_g and ^2A_u, respectively, it is clear that the two experimentally observed ESA bands for D_2 and D_1 must stem from transitions to different excited states which we denote D_N and D_M (Figure 6). With the experimental and

theoretical data for the excited states of the $Car^{\bullet+}$, one arrives finally at a kinetic model for the observed excited-state dynamics upon excitation of the D_3 electronic state, which is displayed in Figure 6. It can be expected that this model is similar for all organic compounds with long chains of conjugated C=C bonds and in particular for all Cars, since the π-electrons determine their spectral features.

Chlorophyll Exited State Quenching by Carotenoid Radical Cations: Implications for NPQ. Recalling the previously proposed NPQ mechanism via electron transfer from a Car to Chl, the electron transfer and the formation of the $Car^{\bullet+}$ were suggested as final quenching step. In view of our findings for the excited-state properties of $Car^{\bullet+}$, in particular their excitation energies and oscillator strengths, new possibilities for Chl fluorescence quenching during NPQ by Cars arise.

Through the formation of the cation, the excitation energies of the neutral Car drop drastically, and most importantly, the strongly allowed D_3 state of the $Car^{\bullet+}$ is clearly lower in energy than the Q_y state of Chl (Figure 6). Thus the $Car^{\bullet+}$ itself can in principle act as terminal quencher of excess excitation energy (EET) via Förster energy transfer $Q_y(Chl) \rightarrow D_3(Car^{\bullet+})$. Moreover, this EET can be expected to be highly efficient due to the large transition dipole moment of the $D_0 \rightarrow D_3$ transition of the $Cars^{\bullet+}$. Once arrived on the $Car^{\bullet+}$, the excess excitation energy is rapidly dissipated according to the internal conversion pathway $D_3 \rightarrow D_2 \rightarrow D_1 \rightarrow D_0$ as identified in our combined experimental and theoretical study (Figure 6).

Thus, this appealingly simple mechanism is an obvious extension of the previously proposed scenario and can be summarized as follows. The first exciton is used to generate the $Car^{\bullet+}$ under NPQ conditions according to Holt et al.[16] The $Car^{\bullet+}$ has been shown to exist for about 150 ps. During its lifetime, however, the cation itself can efficiently act as quencher accepting excitation energy from neighboring excited Chls and dissipate it into heat within 10 ps. If the $Car^{\bullet+}$ is isolated or the excitation level is low, the effect is negligible but when the $Car^{\bullet+}$ is tightly coupled to the other pigment molecules, it acts as an energy sink and quenches excess excitation energy of the entire coupled unit. In light harvesting complexes the pigments are in fact tightly packed and strongly coupled, which ensures not only efficient light absorption per unit volume but also increases the ease of photoprotection.

So far, the proposed extension of the electron transfer mechanism is motivated by our findings for isolated $Car^{\bullet+}$. It is appealing and obvious; however, it still awaits experimental verification in light harvesting complexes, that is, in the natural environment. Thus, we plan to perform a pump probe experiment in the near future studying the excited-state lifetime of Chls of light harvesting complexes in the presence of $Car^{\bullet+}$. Preliminary results indicate already a substantial drop of the Chl excited-state lifetime when $Car^{\bullet+}$ are generated in light harvesting complexes of plants by resonant two-photon two-color ionization. However, these first results require further corroboration and clarification.

Brief Summary

In a combined experimental and theoretical investigation employing femtosecond TA spectroscopy and quantum chemical calculations, the excited states of the radical cations of Lut and β-Car and their properties have been investigated. The absorption wavelengths of the electronic excitations are demonstrated to depend on the polarizability of the solvent and on the number of conjugated double bonds of the Cars. Most importantly, our results undoubtedly reveal the existence of two low-lying excited states below the well-known excited-state absorbing in the near-IR region. In analogy to neutral Cars possessing a strongly allowed S_2 state, this state has been denoted as D_2 state in $Car^{\bullet+}$, but based on our study we propose to refer to it as D_3 in the future. The three energetically lowest states of the $Car^{\bullet+}$ possess $\pi\pi^*$ character and have ^2B_g (D_1, D_3) and ^2A_u (D_2) pseudosymmetry in C_{2h}. Since the electronic ground-state has also ^2A_u pseudosymmetry, the D_2 state is one-photon forbidden, while D_1 has a small oscillator strength and D_3 is strongly allowed with a very large oscillator strength. In comparison with the excitation energies of neutral Cars, the excited states of $Car^{\bullet+}$ are shifted to substantially lower energies resulting in much smaller excitation energies. The lifetimes of the excited states of the $Car^{\bullet+}$ are short and exhibit values of 1.3, 6, and 12 ps for the D_3, D_2, and D_1 states of $Lut^{\bullet+}$ and 0.8, 3.6, and 9.4 ps for the corresponding states of β-$Car^{\bullet+}$. Similar to neutral Cars, the excited-state lifetimes decrease with increasing number of the conjugated double bonds. These findings have important consequences for the ability to quench excited states of Chls via Förster energy transfer and thus for the role of $Car^{\bullet+}$ in NPQ. In view of our findings, $Car^{\bullet+}$ are most likely not generated via electron transfer from Car to Chl as final quenching product during NPQ but instead are formed as active quenching site, since they can efficiently accept excitation energy from Chl due to the low excitation energy and large oscillator strength of their D_3 state. In addition $Car^{\bullet+}$ can rapidly dissipate the excitation energy within 15 ps.

Acknowledgment. This work has been supported by the SFB 472 ("Molecular Bioenergetics"), as well as by the CEF "Macromolecular Complexes" of the University of Frankfurt. A.D. is supported by the Deutsche Forschungsgemeinschaft as an "Emmy Noether" fellow.

References and Notes

(1) Foote, C. S. *Science* **1968**, *162*, 963.
(2) Foote, C. S.; Chang, Y. C.; Denny, R. W. *J. Am. Chem. Soc.* **1970**, *92*, 5216.
(3) Griffiths, M.; Sistrom, W. R.; Cohenbazire, G.; Stanier, R. Y. *Nature* **1955**, *176*, 1211.
(4) Niyogi, K. K. *Ann. Rev. Plant Physiol. Plant Mol. Biol.* **1999**, *50*, 333.
(5) Renger, G.; Wolff, C. *Biochim. Biophys. Acta* **1977**, *460*, 47.
(6) Frank, H. A.; Cogdell, R. J. *Photochem. Photobiol.* **1996**, *63*, 257.
(7) Polivka, T.; Sundstrom, V. *Chem. Rev.* **2004**, *104*, 2021.
(8) Edge, R.; McGarvey, D. J.; Truscott, T. G. *J. Photochem. Photobiol., B* **1997**, *41*, 189.
(9) Seddon, J. M.; Ajani, U. A.; Sperduto, R. D.; Hiller, R.; Blair, N.; Burton, T. C.; Farber, M. D.; Gragoudas, E. S.; Haller, J.; Miller, D. T.; Yannuzzi, L. A.; Willett, W. *JAMA, J Am. Med. Assoc.* **1994**, *272*, 1413.
(10) Horton, P.; Ruban, A. V.; Walters, R. G. *Ann. Rev. Plant Physiol. Plant Mol. Biol.* **1996**, *47*, 655.
(11) Muller, P.; Li, X. P.; Niyogi, K. K. *Plant Physiol.* **2001**, *125*, 1558.
(12) Amarie, S.; Standfuss, J.; Barros, T.; Kühlbrandt, W.; Dreuw, A.; Wachtveitl, J. *J. Phys. Chem. B* **2007**, *111*, 3481.
(13) Avenson, T. J.; Ahn, T. K.; Zigmantas, D.; Niyogi, K. K.; Li, Z.; Ballottari, M.; Bassi, R.; Fleming, G. R. *J. Biol. Chem.* **2007**, 3550.
(14) Bode, S.; Quentmeier, C. C.; Liao, P. N.; Barrosc, T.; Walla, P. J. *Chem. Phys. Lett.* **2008**, *450*, 379.
(15) Dreuw, A.; Wormit, M. *J. Inorg. Biochem.* **2008**, *102*, 458.
(16) Holt, N. E.; Zigmantas, D.; Valkunas, L.; Li, X. P.; Niyogi, K. K.; Fleming, G. R. *Science* **2005**, *307*, 433.
(17) Ruban, A. V.; Berera, R.; Ilioaia, C.; van.Stokkum, I. H. M.; Kennis, J. T. M.; Pascal, A. A.; van Amerongen, H.; Robert, B.; Horton, P.; van Grondelle, R. *Nature* **2007**, *450*, 575.
(18) Standfuss, R.; van Scheltinga, A. C. T.; Lamborghini, M.; Kühlbrandt, W. *EMBO J.* **2005**, *24*, 919.
(19) Ahn, T. K.; Avenson, T. J.; Ballottari, M.; Cheng, Y. C.; Niyogi, K. K.; Bassi, R.; Fleming, G. R. *Science* **2008**, *320*, 794.
(20) Pascal, A. A.; Liu, Z. F.; Broess, K.; van Oort, B.; van Amerongen, H.; Wang, C.; Horton, P.; Robert, B.; Chang, W. R.; Ruban, A. *Nature* **2005**, *436*, 134.

(21) Dreuw, A.; Fleming, G. R.; Head-Gordon, M. *Biochem. Soc. Trans.* **2005**, *33*, 858.
(22) Polivka, T.; Pullerits, T.; Frank, H. A.; Cogdell, R. J.; Sundstrom, V. *J. Phys. Chem. B* **2004**, *108*, 15398.
(23) Polivka, T.; Zigmantas, D.; Herek, J. L.; He, Z.; Pascher, T.; Pullerits, T.; Cogdell, R. J.; Frank, H. A.; Sundstrom, V. *J. Phys. Chem. B* **2002**, *106*, 11016.
(24) Fungo, F.; Otero, L.; Durantini, E.; Thompson, W. J.; Silber, J. J.; Moore, T. A.; Moore, A. L.; Gust, D.; Sereno, L. *Phys. Chem. Chem. Phys.* **2003**, *5*, 469.
(25) Moore, T. A.; Gust, D.; Mathis, P.; Mialocq, J. C.; Chachaty, C.; Bensasson, R. V.; Land, E. J.; Doizi, D.; Liddell, P. A.; Lehman, W. R.; Nemeth, G. A.; Moore, A. L. *Nature* **1984**, *307*, 630.
(26) Savolainen, J.; Dijkhuizen, N.; Fanciulli, R.; Liddell, P. A.; Gust, D.; Moore, T. A.; Moore, A. L.; Hauer, J.; Buckup, T.; Motzkus, M.; Herek, J. L. *J. Phys. Chem. B* **2008**, *112*, 2678.
(27) Frank, H. A.; Brudvig, G. W. *Biochemistry* **2004**, *43*, 8607.
(28) Tracewell, C. A.; Brudvig, G. W. *Biochemistry* **2003**, *42*, 9127.
(29) Huber, R.; Satzger, H.; Zinth, W.; Wachtveitl, J. *Opt. Commun.* **2001**, *194*, 443.
(30) Lenz, M. O.; Huber, R.; Schmidt, B.; Gilch, P.; Kalmbach, R.; Engelhard, M.; Wachtveitl, J. *Biophys. J.* **2006**, *91*, 255.
(31) Parr, R. G. and Yang, W. in *Density-functional Theory of Atoms and Molecules* (International Series of Monographs on Chemistry, Vol. 16) Oxford University Press, 1989.
(32) Casida, M. E. in D. P. Chong (Ed.), *Recent Advances in Density Functional Methods, Part I* (Recent Advances in Computational Chemistry, Vol.1) World Scientific, Singapore, 1995; Vol. 155.
(33) Dreuw, A.; Head-Gordon, M. *Chem. Rev.* **2005**, *105*, 4009.
(34) Becke, A. D. *J. Chem. Phys.* **1993**, *98*, 5648.
(35) Shao, Y.; Molnar, L. F.; Jung, Y.; Kussmann, J.; Ochsenfeld, C.; Brown, S. T.; Gilbert, A. T. B.; Slipchenko, L. V.; Levchenko, S. V.; O'Neill, D. P.; DiStasio, R. A.; Lochan, R. C.; Wang, T.; Beran, G. J. O.; Besley, N. A.; Herbert, J. M.; Lin, C. Y.; Van.Voorhis, T.; Chien, S. H.; Sodt, A.; Steele, R. P.; Rassolov, V. A.; Maslen, P. E.; Korambath, P. P.; Adamson, R. D.; Austin, B.; Baker, J.; Byrd, E. F. C.; Dachsel, H.; Doerksen, R. J.; Dreuw, A.; Dunietz, B. D.; Dutoi, A. D.; Furlani, T. R.; Gwaltney, S. R.; Heyden, A.; Hirata, S.; Hsu, C. P.; Kedziora, G.; Khalliulin, R. Z.; Klunzinger, P.; Lee, A. M.; Lee, M. S.; Liang, W.; Lotan, I.; Nair, N.; Peters, B.; Proynov, E. I.; Pieniazek, P. A.; Rhee, Y. M.; Ritchie, J.; Rosta, E.; Sherrill, C. D.; Simmonett, A. C.; Subotnik, J. E.; Woodcock, H. L.; Zhang, W.; Bell, A. T.; Chakraborty, A. K.; Chipman, D. M.; Keil, F. J.; Warshel, A.; Hehre, W. J.; Schaefer, H. F.; Kong, J.; Krylov, A. I.; Gill, P. M. W.; Head-Gordon, M. *Phys. Chem. Chem. Phys.* **2006**, *8*, 3172.
(36) Grana, A. M.; Lee, T. J.; Head-Gordon, M. *J. Phys. Chem.* **1995**, *99*, 3493.
(37) Head-Gordon, M.; Grana, A. M.; Maurice, D.; White, C. A. *J. Phys. Chem.* **1995**, *99*, 14261.
(38) Starcke, J. H.; Wormit, M.; Schirmer, J.; Dreuw, A. *Chem. Phys.* **2006**, *329*, 39.
(39) Tavan, P.; Schulten, K. *Phys. Rev. B* **1987**, *36*, 4337.
(40) Schirmer, J.; Trofimov, A. B. *J. Chem. Phys.* **2004**, *120*, 11449.
(41) Trofimov, A. B.; Schirmer, J. *J. Phys. B: At. Mol. Opt. Phys.* **1995**, *28*, 2299.
(42) Fujii, R.; Koyama, Y.; Mortensen, A.; Skibsted, L. H. *Chem. Phys. Lett.* **2000**, *326*, 33.
(43) Gurzadyan, G. G.; Steenken, S. *Phys. Chem. Chem. Phys.* **2002**, *4*, 2983.
(44) Zhang, J. P.; Fujii, R.; Koyama, Y.; Rondonuwu, F. S.; Watanabe, Y.; Mortensen, A.; Skibsted, L. H. *Chem. Phys. Lett.* **2001**, *348*, 235.
(45) Jeevarajan, J. A.; Wei, C. C.; Jeevarajan, A. S.; Kispert, L. D. *J. Phys. Chem.* **1996**, *100*, 5637.
(46) Polyakov, N. E.; Leshina, T. V.; Salakhutdinov, N. F.; Kispert, L. D. *J. Phys. Chem. B* **2006**, *110*, 6991.
(47) Bautista, J. A.; Tracewell, C. A.; Schlodder, E.; Cunningham, F. X.; Brudvig, G. W.; Diner, B. A. *J. Biol. Chem.* **2005**, *280*, 38839.
(48) Andersson, P. O.; Gillbro, T.; Ferguson, L.; Cogdell, R. J. *Photochem. Photobiol.* **1991**, *54*, 353.
(49) Galinato, M. G.; Niedzwiedzki, D.; Deal, C.; Birge, R. R.; Frank, H. A. *Photosynth. Res.* **2007**, *94*, 67.
(50) Bally, T.; Nitsche, S.; Roth, K.; Haselbach, E. *J. Am. Chem. Soc.* **1984**, *106*, 3927.
(51) Papagiannakis, E.; Vengris, M.; Larsen, D. S.; van Stokkum, I. H. M.; Hiller, R. G.; van Grondelle, R. *J. Phys. Chem. B* **2006**, *110*, 512.
(52) Niedzwiedzki, D. M.; Sullivan, J. O.; Polivka, T.; Birge, R. R.; Frank, H. A. *J. Phys. Chem. B* **2006**, *110*, 22872.
(53) Buckup, T.; Savolainen, J.; Wohlleben, W.; Herek, J. L.; Hashimoto, H.; Correia, R. R. B.; Motzkus, M. *J. Chem. Phys.* **2006**, 125.
(54) Dreuw, A.; Weisman, J. L.; Head-Gordon, M. *J. Chem. Phys.* **2003**, *119*, 2943.
(55) Dreuw, A.; Head-Gordon, M. *J. Am. Chem. Soc.* **2004**, *126*, 4007.
(56) Kawashima, Y.; Nakayama, K.; Nakano, H.; Hirao, K. *Chem. Phys. Lett.* **1997**, *267*, 82.

JP806030Y